

# Evaluation and Analysis Techniques of Transformer Performances in JFE Steel

OMURA Takeshi<sup>\*1</sup> INOUE Hirotaka<sup>\*2</sup> YAMAGUCHI Hiroi<sup>\*3</sup>

## Abstract:

*Local analysis techniques were used to investigate the iron loss and noise generation mechanism of the transformer. The interlaminar flux between the cores had a large effect on the iron loss of the three-legged wound transformer core. In the lap core having the joint part, the interlaminar flux was larger than that in the non-cut core having no joint part. The reason is that the flux flows to avoid the joint part of the inner core. From the results of 3D vibration analysis of the three-legged stacked transformer core, it was considered that the out-of-plane vibration was the main cause of the acoustic noise, because the largest vibration was the out-of-plane vibration, which was several tens of times as large as calculated from the magnetostriction.*

## 1. Introduction

Grain-oriented electrical steel manufactured by JFE Steel is mainly used in transformer cores for electric power, and is an important material which is directly related to the performance of the transformers. Improvement of the properties of this grain-oriented electrical steel has improved transformer iron loss, and has also reduced transformer acoustic noise. However, there are high needs for improvement of transformer performance. In particular, further reduction of iron loss and acoustic noise are demanded.

In order to reduce transformer iron loss, it is important not only to reduce the iron loss of the core materials, but also to prevent increased iron loss when those materials are assembled as a transformer. The ratio of transformer iron loss in comparison with the steel sheet materials is called the building factor (B.F.), and a small B.F. is generally desired. In stacked transformer cores, increases in B.F. are considered to originate from rotating magnetic flux<sup>1)</sup>, the flow of magnetic

flux to avoid joints that occurs in the T-joint area of the core, partial concentrations of magnetic flux, and interlaminar flux between the stacked steel sheets<sup>2)</sup>. Moreover, in wound transformer cores, the causes of increased B.F. are said to include perpendicular flows of flux to neighboring steel sheets in sheet lap areas<sup>3,4)</sup> and concentration of magnetic flux to the inner core<sup>5)</sup>. Measurement of the local magnetization behavior in the core and quantitative evaluation of the effects of the above-mentioned factors is extremely effective for discovering methods to reduce B.F.

In this paper, the effects on B.F. of the interlaminar flux between cores that is considered to occur in three-legged wound transformer cores, in which the two inner cores are surrounded by an outer core, were evaluated by local magnetization measurements using a search coil and local iron loss measurements using the infrared thermography method<sup>6)</sup> established by Yamaguchi *et al.* The evaluation results<sup>7)</sup> are described in Chapter 2.

On the other hand, transformer acoustic noise is considered to originate from magnetostriction (minute expansion/contraction of the steel sheets accompanying magnetization) and vibration caused by the electromagnetic forces generated between the steel sheets, and is affected by the natural vibration characteristics of the elements that make up a transformer. The relationship between magnetostrictive vibration and acoustic noise<sup>8,9)</sup> and the effect of the magnetic flux density distribution on magnetostrictive vibration<sup>2,10)</sup> have been reported. Magnetostrictive vibration is thought to cause acoustic noise by way of core vibration. Therefore, in order to discover an effective method for reducing acoustic noise, it is considered important to clarify the relationships between magnetostriction and core vibration and between core vibration and acoustic noise before making a direct relationship between magnetostriction and acoustic noise.

<sup>†</sup> Originally published in *JFE GIHO* No. 52 (Aug. 2023), p. 47–54

<sup>\*1</sup> Senior Researcher Deputy General Manager,  
Electrical Steel Research Dept., Steel Res. Lab., JFE Steel

<sup>\*2</sup> Senior Researcher Deputy Manager,  
Electrical Steel Research Dept., Steel Res. Lab., JFE Steel

<sup>\*3</sup> Dr. Eng., Senior Researcher General Manager,  
Electrical Steel Research Dept., Steel Res. Lab., JFE Steel

In this paper, Chapter 3 describes the results of an investigation of the series of behaviors (single sheet magnetostriction and stacked magnetostriction, stacked magnetostriction and core vibration, core vibration and acoustic noise) by which the magnetostriction of a single sheet is changed into acoustic noise characteristics by 3D vibration analysis using laser Doppler vibrometry and strain gauges<sup>11)</sup>.

## 2. Effect of Interlaminar Flux between Cores on Iron Loss of Three-Legged Wound Transformer Core

### 2.1 Experimental Method

Cores with the outer dimensions shown in **Fig. 1** were prepared using grain-oriented electrical steel with a thickness of 0.23 mm as the core material, and stress relief annealing was performed.

In order to investigate the effect of joints of the steel sheets, here, lap cores in which the sheets were joined by lap joints, and non-cut cores with the same geometry but with no sheet cut areas were prepared. In the lap joining method, the lapped length of pairs of steel sheets was 8 mm, and a 1-sheet lap, 7-step lap joint was used.

In the evaluation of the interlaminar flux between the cores, the local magnetic measurement method by search coils was used. To calculate the interlaminar flux between the cores from the difference in the magnetic flux in each part of the cores, search coils were arranged at the positions shown in **Fig. 2**, and the flux at each position was measured by the electromotive

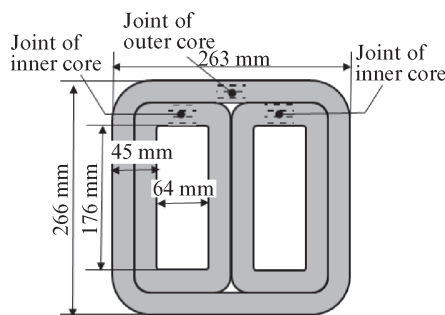


Fig. 1 Dimensions of model transformer core

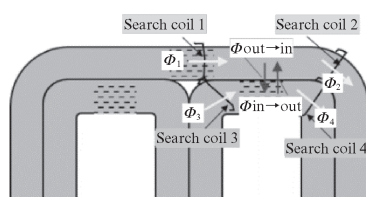


Fig. 2 Position of search coils and schematic image of magnetic flux

force generated in the search coils. The flux from the outer core to the inner core was derived from the difference between search coil 1 and search coil 2 on the outer core, while the flux from the inner core to the outer core was derived from the difference between search coils 3 and 4 on the inner core, and their average value  $\Phi_{\text{interlaminar}}$  was taken as the interlaminar flux between the cores.

Next, in the evaluation of the distribution of iron loss in the interior of the core, a local temperature measurement method using an infrared thermography camera was used. The local iron loss  $P$  of a core is given by its rate of temperature increase  $dT/dt$  and specific heat  $C$ , as shown in Eq. (1).

$$P = C \times \frac{dT}{dt} \dots\dots\dots (1)$$

**Figure 3** shows the excitation pattern used when obtaining the rate of temperature increase  $dT/dt$ . The following were performed in the respective steps in Fig. 3.

- (I) Acquisition of the background of the temperature distribution image before excitation.
- (II) Rapid voltage increase to the specified magnetic flux density.
- (III) Holding at the specified magnetic flux density, and derivation of the average value of the rate of temperature increase.
- (IV) Disconnecting the circuit by instantly setting the excitation voltage to zero.

### 2.2 Experimental Results and Discussion

**Figure 4** shows the results of the measurements of the interlaminar flux between cores  $\Phi_{\text{interlaminar}}$  of the non-cut core and the lap core at the maximum magnetic flux density of 1.7 T and frequency of 50 Hz. The phase was defined as zero at the timing when the magnetic flux density of the left leg reached its maximum value. In both cores, the largest interlaminar flux from

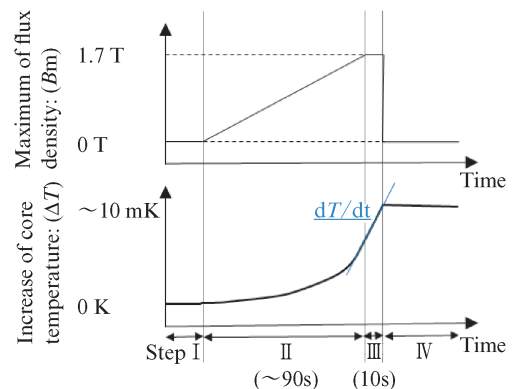


Fig. 3 Schematic pattern of excitation and temperature rise in thermography measurement

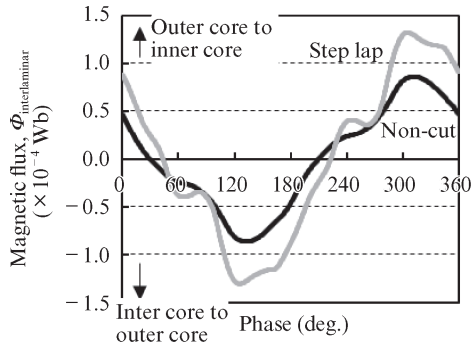


Fig. 4 Interlaminar flux between inner and outer core in non-cut core and lap core

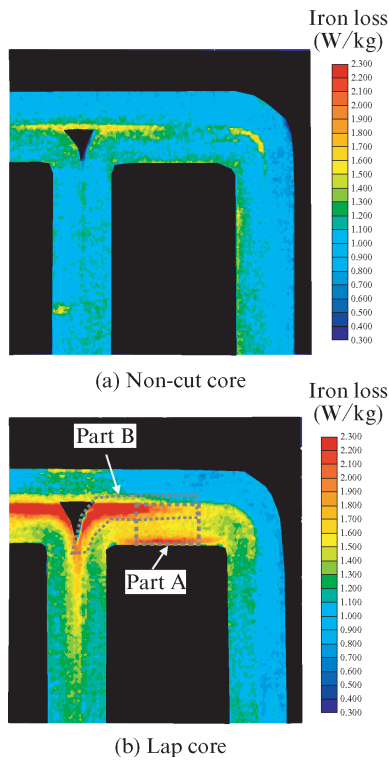


Fig. 5 Distribution of iron loss in core derived from temperature rise

the inner core to the outer core occurred at the phase of  $120^\circ$ , and the largest interlaminar flux from the outer core to the inner core occurred at the phase of  $300^\circ$ . In both cases, the interlaminar flux of the lap core was approximately 1.5 times larger than that of the non-cut core.

**Figure 5** shows the local iron loss distribution of the non-cut core and the lap core at the maximum magnetic flux density of 1.7 T and frequency of 50 Hz. Here, the average values of iron loss of the entire core were corrected to show the iron loss measured by a wattmeter. The iron loss of the inner core was large in both the non-cut core and the lap core. Comparing the two cores, in the lap core, iron loss was large in the lap joint area (Part A) and the outermost part of the inner

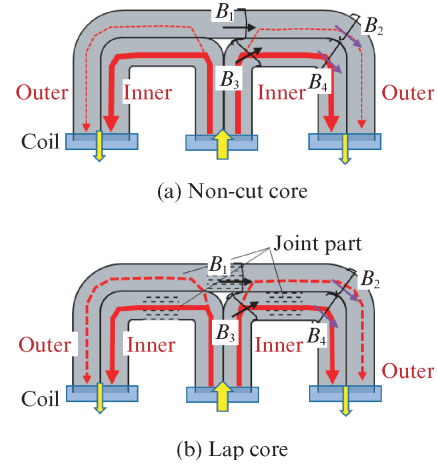


Fig. 6 Schematic image of magnetic fluxes in non-cut and lap cores

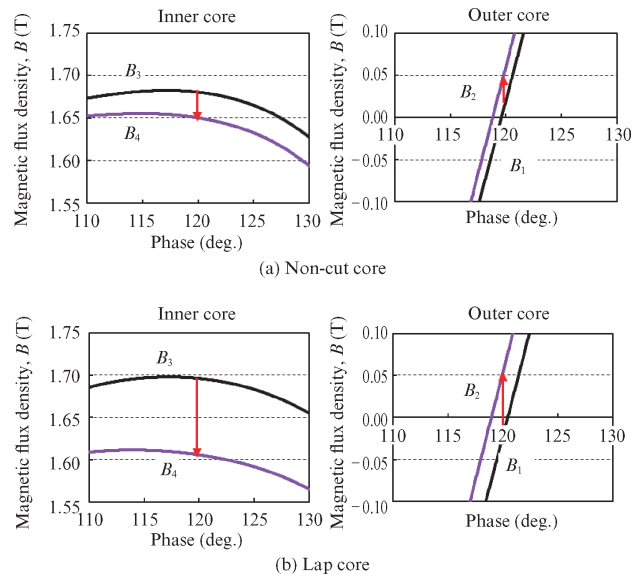


Fig. 7 Comparison of magnetic flux densities between center limb and right limb

core on the center leg side (Part B). The ratios of the increase in iron loss of Part A and Part B to the average iron loss of the entire core were 1.4 times for Part A and 1.8 times for Part B. Therefore, it can be understood the increase in iron loss in these parts is that the main factor in the increase in B.F.

**Figure 6** shows an estimated diagram of the flux flows at the phase difference of  $120^\circ$ . At the  $120^\circ$  phase difference, the largest flux occurs in the center leg, while the fluxes in the right and left legs flow in the opposite direction to that of the center leg and seem to be about half of that in the center leg. **Figure 7** shows the change over time of the magnetic flux densities of the inner core and outer core at the yoke parts of the center leg and right leg at the maximum magnetic flux

density of 1.7 T and frequency of 50 Hz. In the non-cut core, the interlaminar flux from the inner core to the outer core between the center leg and right leg was small, at about 0.03 T. In contrast, the interlaminar flux flow in the lap core was large, at 0.08 T. Since a lap joint with large magnetic reluctance exists in the magnetic path in the inner core, it is thought that this large interlaminar flux flow occurs because the flux flow from the inner core to the outer core increases so as to avoid the lap area.

The increase in the iron loss at the outermost part of the inner core in the center limb of the lap core (Part B in Fig. 5) is considered to be due to the generation of in-plane eddy current loss by the interlaminar flow and local concentration of the magnetic flux when avoiding the lap area. Therefore, in the future, it will be necessary to study the relationship between the interlaminar flux between sheets and in-plane eddy current loss by both numerical analysis and an experimental approach.

### 3. 3D Vibration Analysis of Three-Legged Stacked Transformer Core

#### 3.1 Experimental Method

Using grain-oriented electrical steel with a thickness of 0.30 mm as the core material, a core with a three-legged core structure and a V-notched yoke was prepared. As the stacking method, a 2-sheet lap, 5-step step lap joint was used. The outer dimension of the core was 500 mm, the total number of stacked sheets was 50, and the weight of the core was approximately 20 kg.

To investigate magnetostrictive vibration in the stacked state, triaxial strain gauges with a gauge length of 5 mm and a rosette ( $0^\circ$ ,  $45^\circ$ ,  $90^\circ$ ) arrangement were attached to the entire core as shown in Fig. 8, and magnetostriction was measured in the 3 phase excitation condition after pressure lamination. Magnetostrictive vibration was defined as magnetostrictive vibration in the sheet normal direction (ND)  $\lambda_{ND}$ , rolling direction (RD)  $\lambda_{RD}$ , and transverse direction (TD)  $\lambda_{TD}$ , and was calculated from  $\lambda_{RD}$  and  $\lambda_{TD}$ , based on the fact that the sum of magnetostriction in these three directions is zero according to the volume conservation law.

Laser Doppler vibrometry was used in the vibration

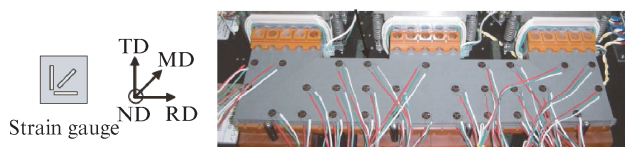


Fig. 8 Arrangement of strain gauges on model transformer core

measurements of the stacked cores. Figure 9 shows the relationship between the laser heads and the steel sheet surface. Reflective blocks (5 mm square) were prepared by affixing reflective tape to the block surface, and were added to the steel sheet surface from measurement holes made in a Bakelite sheet. Measurement by laser irradiation from the direction perpendicular to the steel sheet surface was possible by arranging the laser heads directly above the blocks to measure the vibration velocity  $V_z$  in the Z direction, and by inserting the laser heads in adjoining non-measurement holes and using mirrors to measure the vibration velocities  $V_x$  and  $V_y$  in the X and Y directions.

In verification using a three-legged stacked transformer core with a capacity of 1 200 kVA, in which grain-oriented steel sheets with a thickness of 0.23 mm were used as the core material, acceleration sensors were attached to the core fixing member, and three-dimensional core vibration was measured. For measurement of acoustic noise, the transformer was placed in an area surrounding by a soundproof wall. Six points on the circumference were measured, and their average value was used in the evaluation.

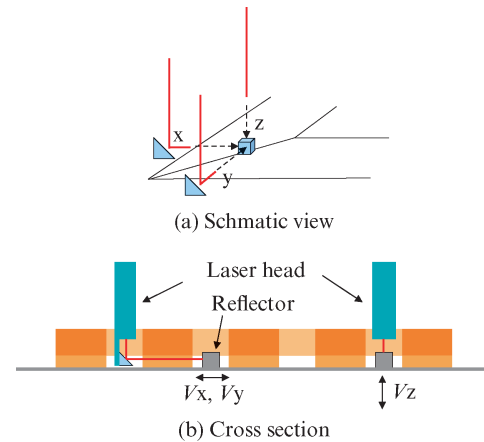


Fig. 9 3D vibration measurement system by using reflective block

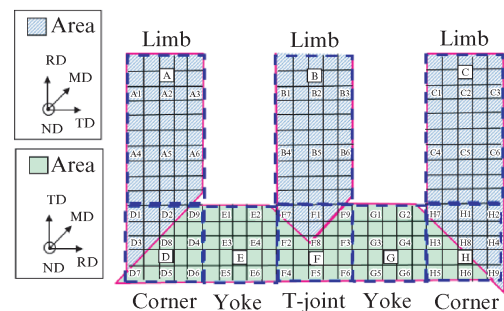


Fig. 10 Measurement point of magnetostriction on model transformer core

### 3.2 Experimental Results and Discussion

Figure 10 shows the magnetostriction measurement points on the model transformer core in the stacked condition. Figure 11 shows the results of the measurements of the magnetostrictive vibration of core in Fig. 10. In comparison with the amplitude of magneto-

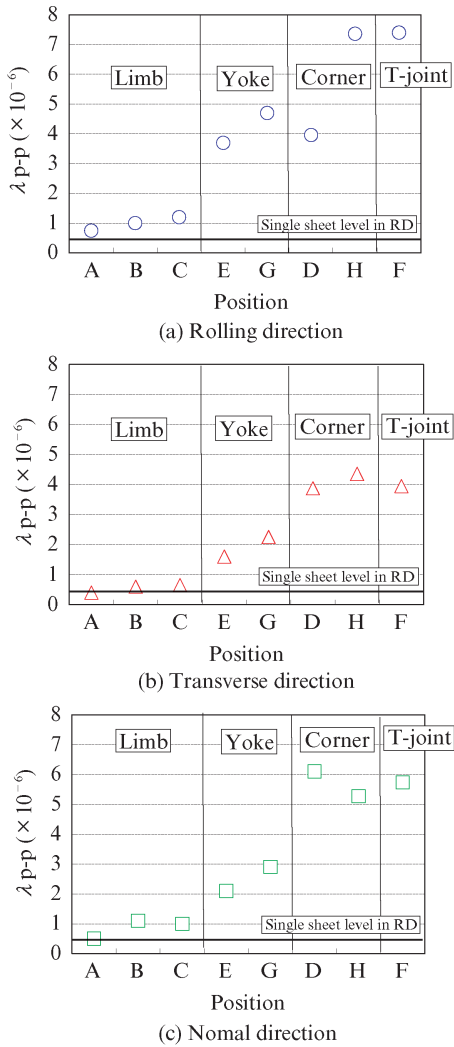


Fig. 11 Amplitude of magnetostriction in each direction on model transformer core

striction in the RD direction in a single sheet, it can be understood that vibration is somewhat larger in the limb part, but is several times or more larger in parts other than the limb. In general grain-oriented electrical steel, it has been reported that the amplitude of magnetostriction under a rotating magnetic flux of 0.7 T is  $5 \times 10^{-6}$  in the RD direction,  $4 \times 10^{-6}$  in the TD direction and  $2 \times 10^{-6}$  in the ND direction<sup>12)</sup>. This amplitude of magnetostriction is several times as large as the amplitude of magnetostriction in the RD direction of a single sheet, and is similar to the amplitude in parts other than the limb in the present experiment. Moreover, a value near 0.7 T has also been reported as the TD direction magnetic component in the vicinity of a joint<sup>13)</sup>. Based on this, the fact that the amplitude of stacked magnetostriction in the yoke, corner and T-joint areas was several times as high as that measured in a single sheet is thought to be caused by rotating magnetization (TD direction).

Next, the parts of the transformer are separated as shown in Fig. 12. Figure 13 shows the maximum displacement in the three directions in each part of this core in the pressurized condition. The number of measurement points in each part was 40 in the limb parts and 25 each in the yoke, corner and T-joint areas. Measurements were made at equal intervals, and the average values of the maximum displacement at each measurement point were taken as the maximum displacement of the respective parts. While in-plane vibration was

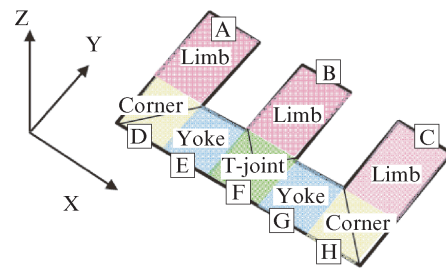


Fig. 12 Measurement point of iron core vibration on model transformer core

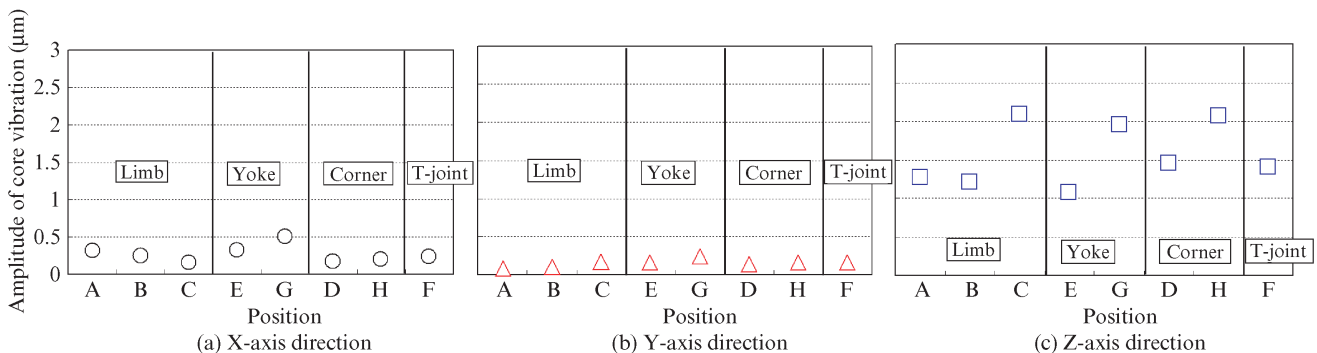


Fig. 13 Amplitude of iron core vibration in each direction on model transformer core



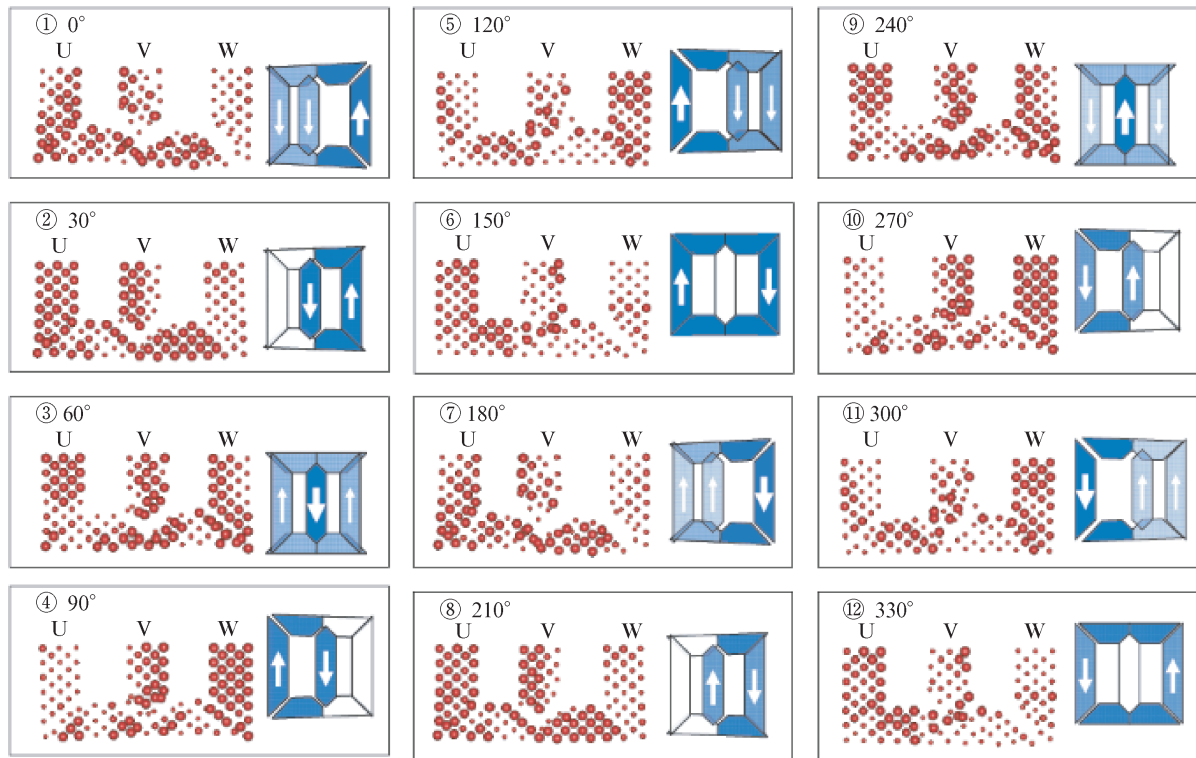


Fig. 14 Vibration behavior of model transformer core

small, out-of-plane vibration was several times as large as in-plane vibration, indicating that the main factor in core vibration is out-of-plane vibration. It is thought that the fact that large out-of-plane vibration was observed even in the limbs, where magnetostrictive vibration is small, may be caused by the effects of magnetostrictive vibration in other parts under the pressurized condition. **Figure 14** shows the vibration displacement in the three directions at each phase angle. The size of the spheres represents the magnitude of out-of-plane vibration, thicker arrows indicate a larger amount of magnetic flux, and the direction of the arrows shows the direction of the magnetic flux. The white regions where arrows are not shown are regions that were not excited. Because out-of-plane vibration reached its maximum at the phase angles of  $30^\circ$  and  $210^\circ$  in the U limb,  $90^\circ$  and  $270^\circ$  in the W limb, and  $150^\circ$  and  $330^\circ$  in the V limb, the maximum displacement occurred under zero excitation in each limb.

In a core, it is thought that magnetization is not simple AC magnetization, even locally, but becomes secondary magnetization with a TD component. **Figure 15** shows a schematic diagram of ideal rotating magnetization. The TD component reaches its maximum at the timing when the magnetization component in the RD direction becomes zero.

The domain structure of grain-oriented electrical steel is formed by stripe-like main domains, which are oriented parallel to the rolling direction, and supplementary domains called lancets. The supplementary domains consist of oblique domains that penetrate through the sheet in the thickness direction in a form that connects these domains with the two spike domains which appear at the top and bottom sides of the sheet<sup>14</sup>.

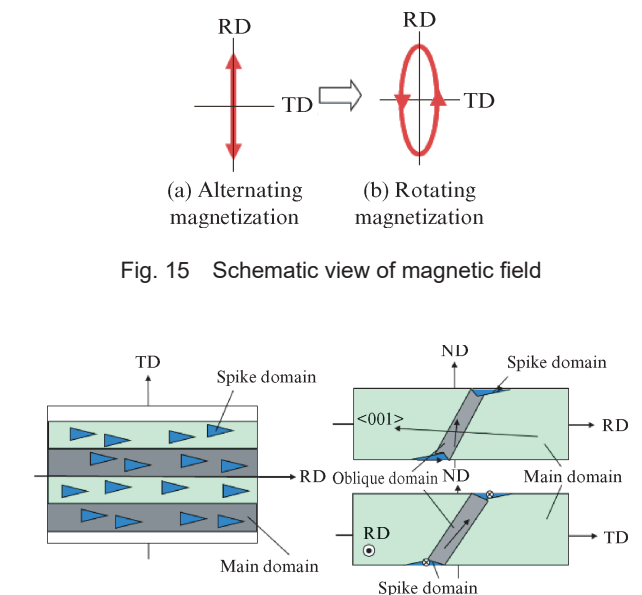


Fig. 15 Schematic view of magnetic field

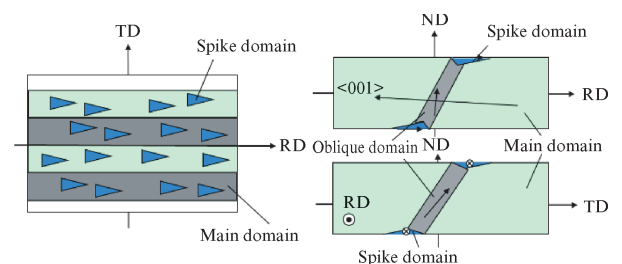


Fig. 16 Magnetic domain model of grain oriented electrical steel

It is known that these domains which penetrate through the sheet thickness direction are located in the plane per-

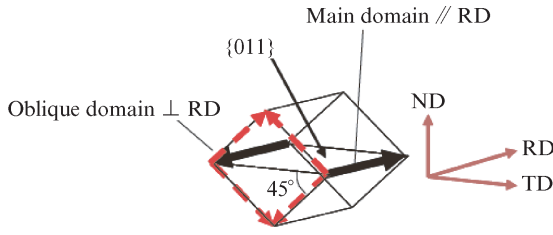


Fig. 17 Magnetic direction of oblique domain vibration amplitude

pendicular to the rolling direction, and their direction of magnetization is oriented at an oblique 45° angle to the sheet surface<sup>12,15)</sup>. Regarding the fact that their direction of magnetization is oriented obliquely in the 45° direction, when the sheet is magnetized in the TD direction, it is thought that the domains that penetrate through the sheet thickness direction, connecting the spike domains, are more active than the main domains, in which the direction of magnetization is the RD direction, and as a result, the sheet expands in the ND and TD directions.

As mentioned above, the largest factor in the core vibration measured in this experiment was out-of-plane vibration. Because this is the timing when the TD direction component is largest, it is thought that the magnetostrictive vibration in the ND direction due to an increase in domains that penetrate through the sheet thickness in a form that connects the spike domains is the cause of out-of-plane vibration of the core.

The amplitude of core vibration (Z direction) and the amount of expansion/contraction (X, Y directions) show the amounts of displacement, and the amplitude of magnetostrictive vibration  $\lambda$  expresses the amount of strain. Therefore, when the sample length is  $L$ , their respective values can be shown by the following equations.

$$\lambda pp = \frac{L_{max} - L_{min}}{L} \dots\dots\dots (2)$$

$$App = L_{max} - L_{min} \dots\dots\dots (3)$$

$$App = \lambda pp \times L \dots\dots\dots (4)$$

Here, the amount of displacement by core vibration in the T-joint area and corner parts that include joints, which are considered to be sources of core vibration, was calculated for the case where the results of the magnetostrictive vibration shown in Fig. 11 become core vibration as-is, and the calculated results were compared with the measured results of core vibration shown in Fig. 13. The comparison of the calculated results and measured results of core vibration is shown in Fig. 18. Although the calculated values and mea-

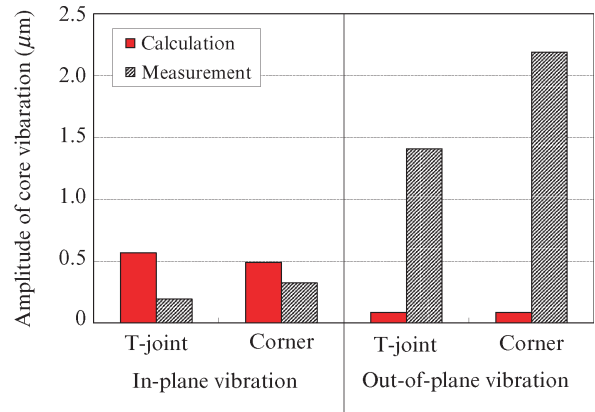


Fig. 18 Comparison of measured values and calculated values by using magnetostriction amplitude in core vibration

sured values for in-plane vibration were comparatively close, large differences between the two could be seen in the results for out-of-plane vibration. From this, it can be said that out-of-plane vibration, which is considered to be the main cause of acoustic noise, increases greatly in comparison with magnetostrictive vibration. In the three-legged stacked transformer core, the excitation in the transformer was not uniform in the width direction of each limb, and magnetization was accompanied by phase differences. Therefore, the conceivable causes of this increase include the possibility that vibration is greatly amplified by the torsional motion caused by the nonuniform magnetostrictive expansion and contraction motions due to this phase difference magnetization, and the possibility that this phenomenon originates from natural vibrational characteristics specific to stacked cores. In an analysis of the vibration characteristics of stacked cores, Mizuno *et al.* noted that the results of an FEM analysis are in good agreement with the measured results if the out-of-plane Young's modulus and in-plane Young's modulus are set to 1/1 000 and 1/10 times the Young's modulus of a silicon steel sheet, respectively, suggesting that stacked cores are particularly susceptible to out-of-plane deformation<sup>16)</sup>.

In the investigation of the model transformer, results showing that out-of-plane (Z direction) vibration of the core has a large effect on acoustic noise were obtained. Next, the results of core vibration in an actual transformer measured with an acceleration sensor will be presented. As shown in Fig. 19, the acceleration sensor was installed at the T-joint area in the upper part of the core. Figure 20 shows the measurement results. Comparing the vibration levels in the three directions, out-of-plane (Z direction) vibration showed the largest vibration level.

Figure 21 shows the relationship between core vibration and acoustic noise in the actual transformer.

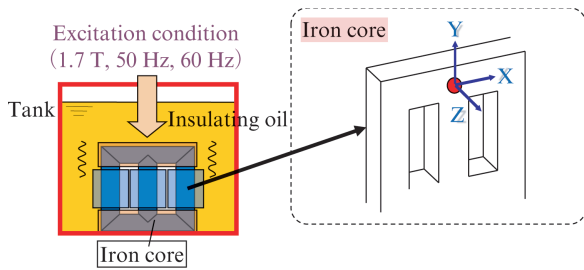


Fig. 19 Measurement point of iron core vibration of oil-filled practical transformer

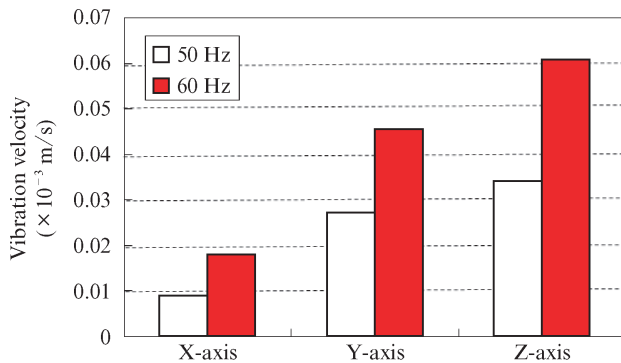


Fig. 20 Measurement result of vibration velocity in each direction on practical transformer core

Hearing sense correction was applied to the core vibration velocity spectra. In the spectra for the X direction, the frequency components showed little change up to approximately 1 500 Hz. Likewise, the spectrum for the Y direction showed changes similar to those of the X direction at the excitation frequency of 60 Hz. Although not as clear as in the X direction, a similar tendency was also observed at the excitation frequency of 50 Hz, in that there was almost no change in the frequency component until 700 to 1 400 Hz. In contrast, in the spectra for the Z direction, the frequency components showed a decreasing tendency as the frequency increased. Looking at the acoustic noise spectrum, the frequency component showed a decreasing tendency as the frequency increased, and the acoustic noise spectrum resembled the spectrum for the Z direction. Based on this as well, core vibration in the vertical direction is considered to have the largest effect on acoustic noise.

#### 4. Conclusion

To materialize low iron loss and low acoustic noise in transformers, it is extremely important to understand the mechanisms of increased iron loss and generation of acoustic noise specific to transformers by utilizing local analysis techniques. From this perspective, the following knowledge was gained through this study.

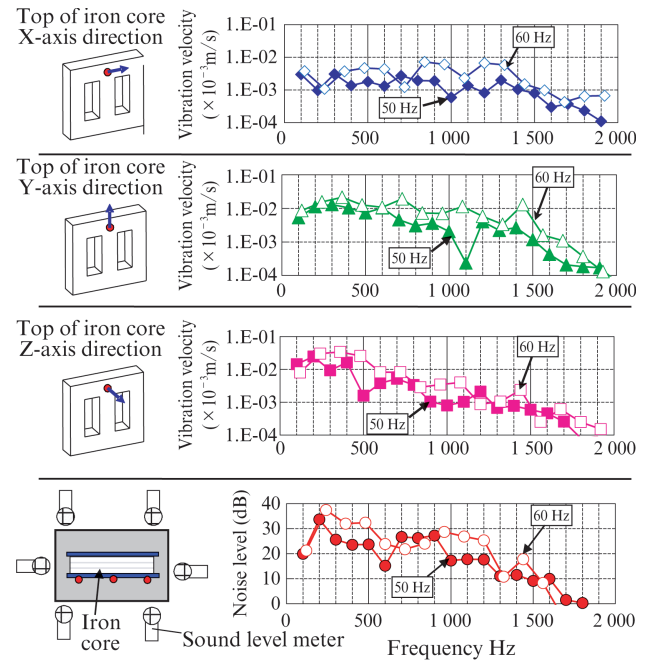


Fig. 21 Power spectrum of core vibration velocity and acoustic noise

- (1) Iron loss in three-legged wound transformers is affected by interlaminar magnetic flux between the iron cores. Interlaminar magnetic flux is larger in lap cores than in non-cut cores because the magnetic flux flows so as to avoid the lap joint area of the inner core.
- (2) In three-legged stacked transformers, the amplitude of vibration in the yoke, corner and T-joint areas is several tens of times as large as the magnetostriction in single sheets. Because the largest factor in core vibration is out-of-plane vibration, this out-of-plane vibration is considered to be the main cause of acoustic noise. In the out-of-plane direction, the measured value of displacement is several tens of times larger than the value predicted from magnetostrictive vibration. The causes of this difference are considered to include the possibility that vibration is greatly amplified by the torsional motion originating from the nonuniform magnetostrictive expansion and contraction motions caused by magnetization accompanying the phase differences that occur in three-phase transformers, and the possibility that vibration is affected by a natural vibration characteristic of the core, namely, susceptibility of the stacked core to out-of-plane deformation.

#### References

- 1) Ishida, M.; Sadahiro, K.; Okabe, S. Analysis of Local Magnetic Properties and Acoustic Noise in Three-Phase Stacked Transformer Core Model. *Kawasaki Steel Giho*. 2003, vol. 35, no. 1, p. 21–27. (in Japanese)
- 2) Yamaguchi, H.; Pfitzner, H.; Ishida, M. 3D Magnetic Flux Measurement in Joint Region of a Model Core Stacked with Grain-Oriented Electrical Steel. *IEEJ Trans. IA*. 2010, vol. 130,



- no. 9, p. 1087–1093. (in Japanese)
- 3) Takakura, Y.; Takahashi, Y.; Fujiwara, K.; Ishihara, Y.; Masuda, T. Iron Loss Analysis of the Wound-Core Transformer Considering Core Joint Configuration. The Papers of Joint Technical Meeting on Static Apparatus and Rotating Machinery. IEE Japan. 2012, SA-12–113, RM-12–128. (in Japanese)
  - 4) Inoue, K.; Harada, K.; Ishihara, Y.; Todaka, T.; Hirakawa, K. The Magnetic Analysis of the Three-phase Transformer with Step-lap Wound-core. The Papers of Technical Meeting on Magnetics. IEE Japan. 1999, MAG-99–174 (in Japanese)
  - 5) M. A. Cinar; B. Alboyaci; M. Sengul. Comparison of Power Loss and Magnetic Flux Distribution in Octagonal Wound Transformer Core Configuration. J. Electr. Eng. Technol. 2014, vol. 9, no. 4, p. 1290–1295.
  - 6) Yamaguchi, H.; Imanishi, D.; Ishida, M.; Inoue, H. Iron Loss Measurement on a Model Transformer Core by Infrared Thermography. The Papers of Technical Meeting on Magnetics. IEE Japan. 2011, MAG-11–129, p. 1–4. (in Japanese)
  - 7) Inoue, H.; Omura, T.; Yamaguchi, H.; Senda, K. Influence of Interlaminar Flux between Cores on Iron Loss in Three-legged Wound Transformer Core. IEEE Trans. FM. 2021, vol. 141, no. 4, p. 226–232.
  - 8) Mizokami, M.; Kubota, T. Properties of Transformer with Stacked Core Applied Steplap Joint. Papers of Technical Meeting on Magnetics. IEE Japan. 1998, MAG-98–173 (in Japanese)
  - 9) Mizokami, M.; Kurosaki, Y. Vibration of Noise and Magnetostriction Associated with Joint Types of Transformer Core. IEEE Trans. FM. 2014, vol. 134, no. 5, p. 334–339. (in Japanese)
  - 10) G. F. Mechler; R. S. Girgis. Magnetic Flux Distribution in Transformer Core Joints. IEEE Trans. Power Delivery. 2000, vol. 15, no. 1, p. 198–203.
  - 11) Omura, T.; Yamaguchi, H.; Ishigaki, Y.; Okabe, S.; Toda, H. 3D Vibration Analysis on Three Phase Transformer Cores. IEEE Trans. FM. 2015, vol. 135, no. 7, p. 414–423.
  - 12) Yamaguchi, H.; Pfützner, H.; Honda, A. Modeling of Magnetic Domain in Grain-oriented Electrical Steel Sheets Based on Multi-directional Magnetostriction Measurements. IEEE Trans. FM. 2010, vol. 130, no. 9, p. 831–836. (in Japanese)
  - 13) Okabe, S.; Ishida, M.; Kurosawa, M. Measurement of Local Magnetic Flux in the T-joint Model of a Three-phase Stacked Transformer Core. J. Magn. Soc. Jpn. 1998, vol. 22, no. 4–2, p. 713–716. (in Japanese)
  - 14) A. Hubert; R. Schafer. Magnetic Domains. 1998, Springer, Berlin
  - 15) Arai, S. Supplementary Magnetic Domains and Magnetic Domain Control of Electrical Steel. J. Magn. Soc. Jpn. 2001, vol. 25, no. 12, p. 1612–1618. (in Japanese)
  - 16) Mizuno, S.; Noda, S.; Min, Z.; Akimoto, K.; Abe, S.; Yamada, S. Natural Vibration Characteristic of Transformer Core. Dynamic & Design Conference. 2011, 702–1”-“702–6” (in Japanese)